# Detection of Foreign Bodies in Food by Thermal Image Processing

Giaime Ginesu, *Student Member, IEEE*, Daniele D. Giusto, *Senior Member, IEEE*, Volker Märgner, *Member, IEEE*, and Peter Meinlschmidt

***Abstract*—This paper deals with the problem of detection of foreign bodies in food. A new method for inspecting food samples is presented, using thermographic images to detect foreign bodies that are not detectable using conventional methods. At first, the basic background of thermography is given. Then, experiments to obtain well-contrasted thermographic images of different food and foreign bodies are discussed. The main part of the present paper introduces specific image processing methods that show a good recognition power of foreign bodies within food. Results achieved with a small set of test images are presented. The results are promising and the methods work even on some poorly contrasted images. To compare the different image processing and recognition methods, a quality index is defined. On the test images the success of the presented methods is shown and the difference in recognition results can be measured using the introduced quality index.**

***Index Terms*—Food inspection, foreign body detection, image processing, nondestructive testing, thermography.**

## I. Introduction

CONSUMERS have high expectations about the purity of food. Food products, therefore, have to be cleaned and prepared to make them suitable for consumption. The industry extensively invests in machinery, processing, and inspection equipment to ensure a high product quality. Unfortunately, in spite of advanced technology and procedures, some contamination will always occur. To overcome this problem the food industry is investigating in all fields of purity control.

This paper refers to the identification of foreign bodies among food products. A foreign body is defined as a piece of solid matter present in a product that is undesirable [10]. The food manufacturer's objective is to supply products completely free from foreign bodies, in order to meet the consumers' expectations.

Manuscript received March 12, 2002; revised May 19, 2003. Abstract published on the Internet January 13, 2004. This work was supported in part by the EU (Socrates/Erasmus programme), by the Forschungskreis der Ernährungsindustrie e.V., Bonn (FEI), by the AiF, and by the German Ministry of Economics and Technology under Project AiF-FV53 ZN. An earlier version of this paper was presented at the IAPR Workshop on Machine Vision Applications, Nara, Japan, December 2002.

G. Ginesu and D. D. Giusto are with the CNIT Multimedia Communications Laboratory, Department of Electrical and Electronic Engineering, University of Cagliari, 09123 Cagliari, Italy (e-mail: g.ginesu@diee.unica.it; ddgiusto@unica.it).

V. Märgner is with the Institute for Communications Technology, Braunschweig Technical University, D-38092 Braunschweig, Germany (e-mail: v.maergner@tu-bs.de).

P. Meinlschmidt is with the Fraunhofer Institute for Wood Research, Wilhelm-Klauditz-Institut, D-38108 Braunschweig, Germany (e-mail: peter.meinlschmidt@wki.fhg.de).

Digital Object Identifier 10.1109/TIE.2004.825286

Visual inspection is usually performed by human operators and its output is then affected by several factors, such as age of operators, their concentration and motivation, fatigue and visual acuity, room conditions (lighting, heating, ventilation, noise, and so on); for these reasons, automated systems are especially welcome.

Many physical separation methods are extensively used to reduce the amount of undesired materials during the production process; these include sieving, elutriation and sedimentation, screening, filtering, air-classification, and gravity systems.

Some more sophisticated detection systems available as practical devices include metal detectors, X-ray machines, and optical sensors. All these detection devices depend on recognizing differences in response to some part of the energy spectrum between a contaminant and the product, but there is no system able to detect every contaminant regardless of size and type.

In previous studies, Pearson *et al.* [1] showed the feasibility of an automated food inspection system for pistachios defects detection based on X-ray imaging and statistical characterization. Talukder *et al.* [2] used X-ray imaging to deal with the problem of nondestructive testing by feature discrimination. Casasent *et al.* [3] obtained promising results by X-ray imaging and neural net processing to classify pistachio nuts. Pearson [4] then used near IR transmittance to detect concealed damage in nuts. Other works deal with the problem of nondestructive quality control by infrared imaging or spectrometry [5]. In this work, we experiment with infrared imaging for the detection of foreign bodies in food products. For image acquisition the system shown in Fig. 1 was used. We focused our attention on the development of appropriate image processing methods to make suitable information available from the acquired data. These techniques were implemented in software and tested on several sample images.

Section II gives a short introduction into the thermographic background. The next section deals with the heat conductivity and heat capacity of real materials and its time-dependent behavior. A description of the experimental setup follows in Section IV. The development of digital image processing algorithms is explained in Section V, and subdivided into binarization, statistical, and morphological methods. Finally, experimental results are given in Section VI.

## II. Thermographic Background

The study of thermal emission by solids starts usually from the concept of a black body, defined as an object capable of absorbing all the incident radiation [6]. The practical realization of a black body consists in building a completely closed cavity, which can be accessed by a hole, with dimensions very small in

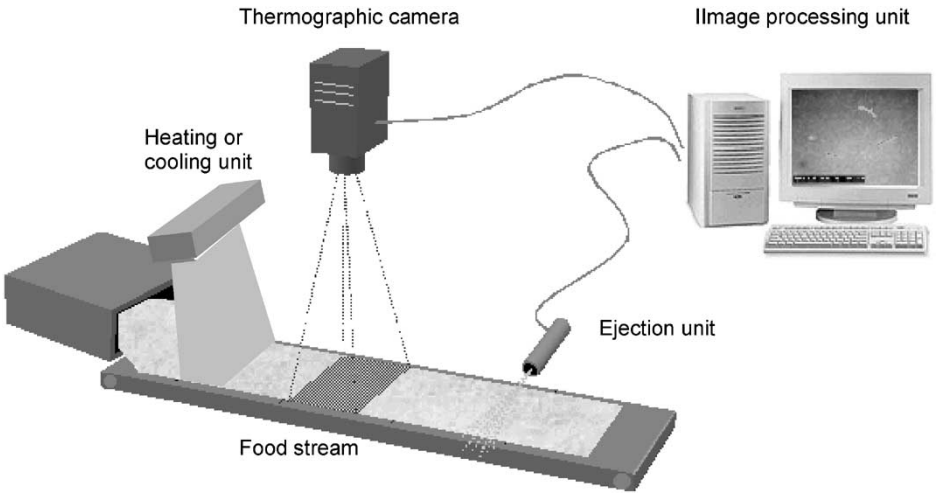


Fig. 1. Example of an inspection system using thermography.

comparison with those of the cavity, characterized by a perfectly absorbing inner surface. Planck's law describes the radiation emission from a black body

$$\frac{\partial R(\lambda,T)}{\partial \lambda} = \frac{2\pi hc^2\lambda^{-5}}{\exp\left(\frac{hc}{\lambda kT}\right)-1} \tag{1}$$

where the first term represents the spectral exitance (the power emitted per unit area and per unit wavelength), $h = 6.6256 \times 10^{-34}$ J·s is Planck's constant, $k = 1.380\,54 \times 10^{-23}$[JK$^{-1}$] is Boltzmann's constant, $c = 2.998 \times 10^{8}$ [ms$^{-1}$] the speed of light, $\lambda$ the wavelength, and $T$ is the absolute temperature in degrees Kelvin.

Usually objects are not black bodies, and the above law does not apply to them without certain corrections. Non-black bodies absorb a fraction $A$, reflect a fraction $R$ and transmit a fraction $T$ of the incident radiation. These fractions are selective, depending on the wavelength and on the angle of incident radiation.

It is necessary to introduce the spectral emissivity $\varepsilon(\lambda)$ to balance the absorbance $A(\lambda)$ so that

$$A(\lambda) = \varepsilon(\lambda) \tag{2}$$

and

$$\varepsilon(\lambda) + R(\lambda) + T(\lambda) = 1. \tag{3}$$

The spectral reflectance of a substance can be expressed in terms of Planck's law as follows:

$$\frac{\partial R(\lambda,T)}{\partial \lambda} = \varepsilon(\lambda)\,\frac{dR_{\text{blackbody}}(\lambda,T)}{\partial \lambda}. \tag{4}$$

That means that the emission coefficient $\varepsilon(\lambda)$ connects the ideal radiation of a black body with real existent objects. A black body is a material that is a perfect emitter of heat energy and has an emissivity value equal to 1. In contrast, a material with zero emissivity would be considered a perfect thermal mirror. However, most real bodies show a wavelength-dependent emissivity like the curves in Fig. 2. If the observed material shows no wavelength-dependent emissivity, the body is called a gray body.

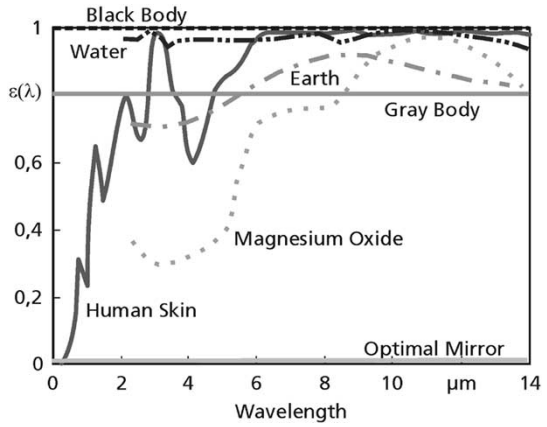


Fig. 2. Emissivity of different materials as a function of the wavelength.

## III. Foreign Body Recognition by Thermography

The possibility of distinguishing between different materials and objects using thermal images depends on different factors. As no real object behaves like a black body, many different phenomena have to be considered to adapt the model accordingly. Some of them are related to mechanical characteristics, such as density, geometric shape, and surface roughness, while others depend on environmental factors like temperature uniformity, lighting, and humidity. Even the relative position of different objects can affect the detection.

Principally there are two different ways to distinguish between food material and foreign bodies by means of thermography, i.e., either by differing emissivities or by using the different heat conductivities or capacities of the materials. If there is a relevant difference in the emissivity coefficient of the materials, as shown for magnesium oxide and human skin at 4 $\mu$m (see Fig. 2), the two materials can be distinguished by infrared radiation. The second method is to apply a heat pulse on the material and to observe the penetration of the heat into the material. The two materials can be distinguished because of the differing heat conductivities.

To perform the recognition process, a well-contrasted image should be obtained, in which the observed gray value differ-

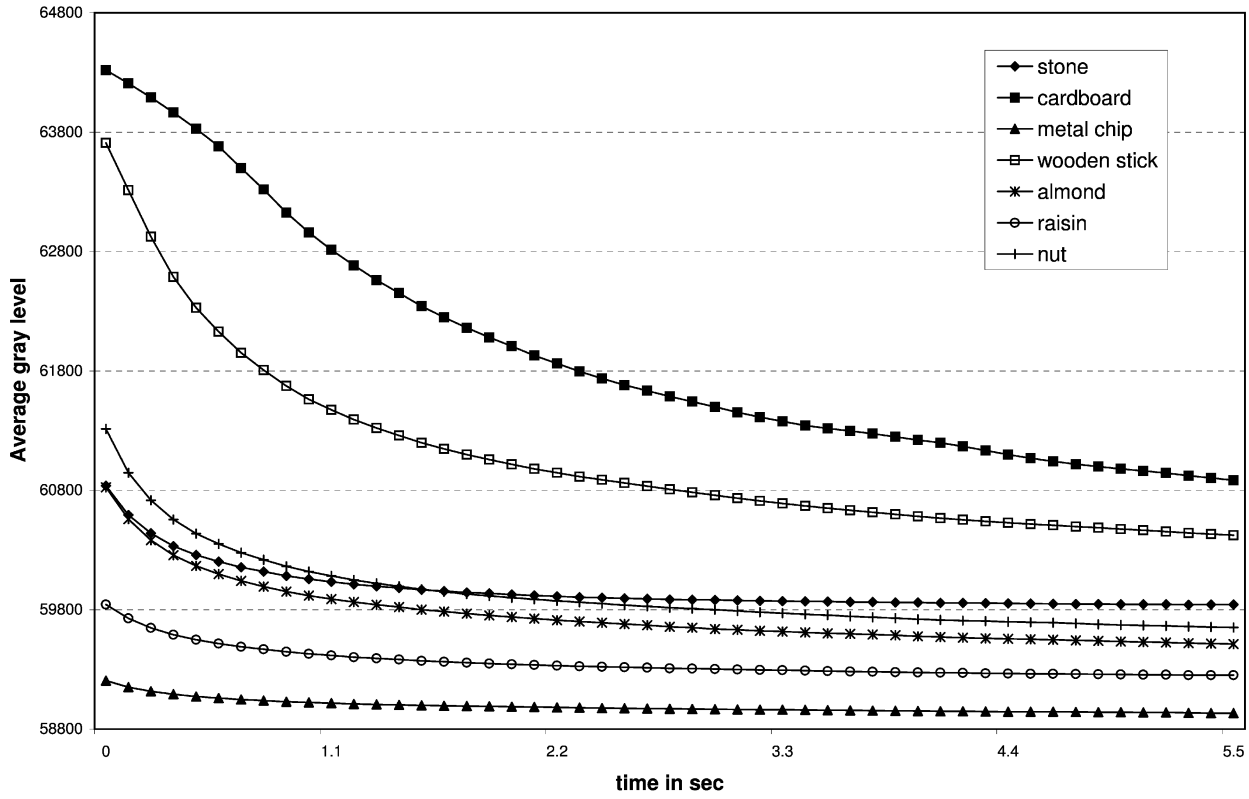


Fig. 3. Decreasing temperature curves of different materials shown as gray levels versus time.

ences between objects and foreign bodies should be as high as possible.

The emissivity of different food and foreign bodies is often not sufficient to get well-contrasted infrared images. To obtain a higher contrast, it is advisable to heat or cool the samples before grabbing the frames. In this case, the differing heating conductivities and capacities cause a different increasing or decreasing behavior of the surface temperature.

Good thermographic images can be achieved using pulse thermography [8]. The basic principle is to leave the object at rest below the infrared (IR) camera, to apply a heat pulse, e.g., produced by a flash light, and to observe the decreasing surface temperature. Because of the different heating conductivities and capacities, the objects will cool down with different speeds. To measure the different heat conductivities a sequence of IR images has to be taken, i.e., shortly enough after the pulse to observe the decreasing temperature of material with high conductivity (e.g., metal) and long enough for materials with low conductivity (e.g., wood).

In our experiments, a long sequence (500 frames, 80 frames/s) has been recorded to extract the data as described above. The acquired sample contains a collection of different materials used to simulate foreign body contamination in real experiments. The average gray level of a $10 \times 10$ pixel neighborhood has been computed for each object along the sequence (Fig. 3).

It is obvious from Fig. 3 that cardboard pieces and wooden sticks behave quite differently from other materials, as they appear much hotter at the beginning and decrease in temperature quickly. This is due to the fact that these materials are dry and light while the fruits contain a big quantity of water (i.e., they heat up more slowly and reach a lower temperature, but maintain the heat for a longer time and cool down slowly). The other materials except metals follow a similar decreasing behavior. In theory, it should heat up and cool down very quickly; in fact, its reflecting surface prevents it from absorbing the heat, resulting in a much flatter characteristic.

By plotting the absolute differences between the previous curves, the temporal behavior of the contrast between different materials is computed (Fig. 4), thus making it possible to distinguish between two materials. When we take wooden sticks, cardboard pieces or metal chips as foreign bodies, the maximum contrast is reached near the beginning of the cooling process. Thus, it is advisable to acquire a frame as soon as possible in the process. On the other hand, stones show the best contrast near the end of the sequence. We can also note that the contrast coming from metal-chip or stone characteristics is much smaller than that of wooden sticks or cardboard pieces. For this reason, foreign body recognition in these cases is expected to be harder.

## IV. Experiment and Instrumentation Characteristics

The thermographic technique should be used to detect foreign bodies at the end of the production chain, when all the other controls, such as sieving or other mechanical devices, have presumably failed. Therefore, it is reasonable to suppose that the foreign bodies constitute a small percentage over the examined product.

Some limitations for the experiments come from the nature of the considered items. Food cannot be treated regardless of

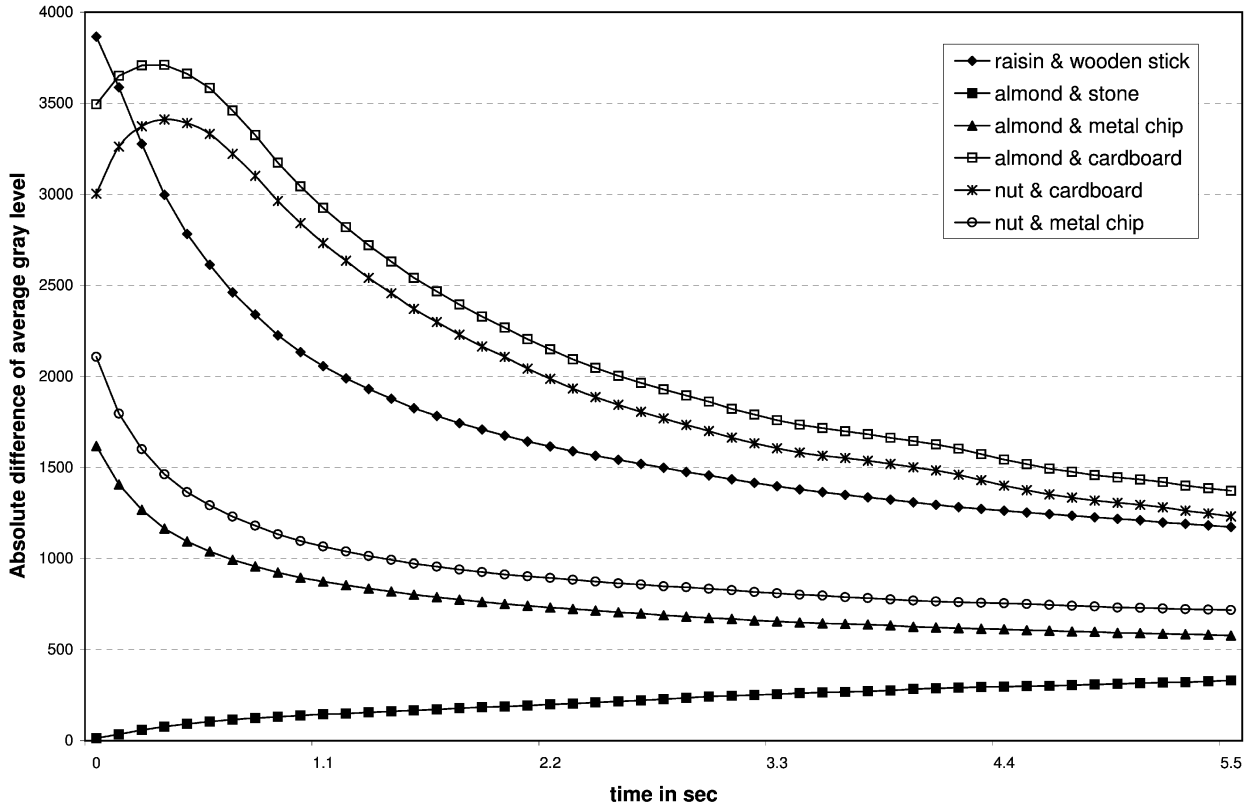


Fig. 4. "Contrast" curves for pairs of food product and foreign bodies shown as absolute difference of gray levels versus time.

its purpose, so it is undesirable to heat the samples to high temperatures. Nonetheless, it would be possible to heat them with microwave antennas. This latter technique can produce well-contrasted images, because microwaves react only with water molecules, but causes additional complications and would require a very precise setting in order not to spoil the sample.

Another limitation comes from the process. In theory, it is possible to obtain very clear images by subtracting the background from the grabbed image (offset correction), thus reducing the noise component considerably. In the real process, however, the apparatus should take images of the material while it is moving on a conveyor belt. In this case, the background is not constant and the background subtraction might cause further undesirable effects. The only way to handle the problem is to consider raw images.

The thermographic apparatus used for the experiments is a Thermosensorik-System CMT 384 M [9]. The camera possesses a matrix of $384 \times 288$ HgCdTe (CMT) cooled infrared sensors, capable of detecting middle infrared radiation in the range of 3.4–5.2 $\mu$m. The temperature resolution is smaller than 15 mK (NETD) and each pixel has a 14-bit resolution. The pixel pitch is $24 \times 24$ $\mu$m and the maximum full frame rate is 80–90 Hz.

## V. Thermographic Image Processing

As our experiments have shown, the thermographic images of food are very different for different materials. Only sometimes a simple gray value threshold can separate the foreign bodies. Usually the whole image is more or less noisy and the detection of the foreign bodies is not that simple.

To solve this problem we implemented a software tool for the interactive selection of the best sequence of image processing operations by testing it on some sample images.

Before analysis and recognition can be done, preprocessing has to be performed in order to enhance the image information content. The preprocessing consists of the following steps: 1) dead pixel correction; 2) first enhancement filter application; 3) second enhancement filter application; 4) shading correction; and 5) histogram stretching.

The first preprocessing task is the correction of dead pixels, defined as those sensor elements in the thermal detecting matrix that behave in an unpredictable way. Such abnormalities, which affect new systems (i.e., at the time of delivery) with a percentage that may reach 1% of total pixels [9], are caused by the destruction of the pixels through cosmic rays, by heat deterioration of sensors and by a high incidence of static electricity, e.g., [7]. Consequently, a perturbation similar to salt and pepper noise is produced, thus heavily affecting the results of the following processing phase and the recognition output. These dead pixels have a constant position on the detector surface and may only increase in number in the course of time. Thus, the easiest way to correct this instrumentation defect is to find all dead pixels and correct their intensity values in the digital image in some way. Dead pixels can be easily found by acquiring two images, one related to a uniformly hot surface, and the other to a cold one; black and white points respectively detected create the array of dead pixels. As the information for each dead pixel is missing, and as it is not possible to predict its correct value, we used a simple operator that substitutes each dead pixel value with a good one chosen in its 8-connected neighborhood (Fig. 5).

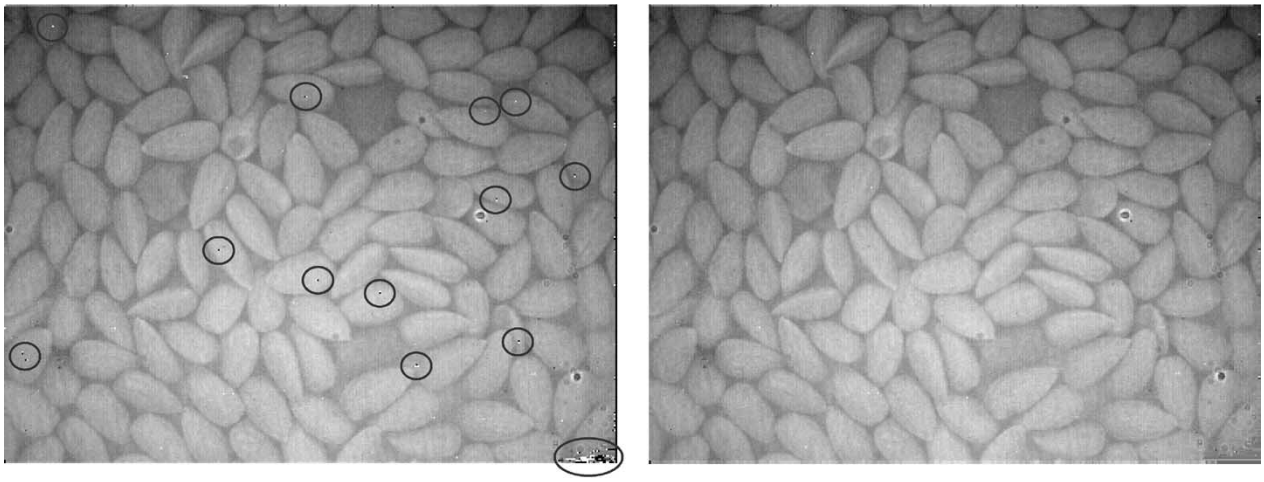

(a) (b)

Fig. 5. IR image of almonds and stones (a) prior to and (b) after the dead pixel correction. The dead pixels are marked by circles.

Afterwards, images are enhanced by a filtering step. We implemented several convolution, rank or morphological filters [11], selectable by the users according to current data characteristic. In many cases, best results can be obtained by applying a median filter (able to despeckle data without loosing fine information), eventually followed by a $3 \times 3$ cross-shaped (morphological) opening operator.

Another undesirable effect comes from shading. In fact, due to nonhomogenous illumination and differing sensitivities between the center and the borders of the sensors, the image can present an inhomogeneous lighting that can lead to severe errors in the following tasks. To avoid this drawback, a background image has to be acquired and subtracted from the original one; it should present slowly varying gray values and its subtraction should not reduce the contrast between background and foreground objects.

Finally, a histogram stretching may be performed for rendering only.

At this point, data are ready to be analyzed and recognized through the scheme that is outlined below. Shortly, three different approaches were designed and tested to solve the problem from different points of view and to fit the majority of occurrences. They rely on binarization, statistical and morphological analysis.

### *A. Adaptive Binarization*

The first approach was developed to classify images with a good contrast, according to real-time constraints. The basic idea is to select a set of starting regions of interest (ROI) and to perform a local analysis aimed at achieving a better recognition on each of them. The main advantage of this method lies in its simplicity and computational speed. This fits our primary objective, i.e., the real-time recognition of objects on a conveyor belt. Moreover, by reducing the observation window to a neighborhood of pixels around the candidate objects, we obtain more stable statistics and reduce noise (i.e., irregular object patterns). Consequently, the automatic determination of the threshold level is more precise and effective.

The main problem of binarization lies in the automatic threshold level determination; at first we tested and used two different methods from the state of the art (discriminant analysis [12] and recursive binarization [15]). Results of both methods show good performance on bimodal histograms. However, as in several cases data do not show a bimodal behavior, a third method was developed to select a histogram "tail" (Fig. 6). This method works well on a unimodal histogram for the food material and some outlier from the foreign bodies.

To identify the starting ROI we developed an adaptive thresholding algorithm. A very discriminating tail-selection thresholding algorithm is first applied to the preprocessed image in order to identify the foreign body candidates. This task can be done by region labeling the resulting image and computing the center of mass for each blob. As a result, we have an array of points identifying the positions of candidate foreign bodies. Starting from these points, we perform local object recognition using a local threshold. We select a square window centered on each center of mass, and iterate the thresholding for each window. In this case, the threshold value is calculated with the discriminant analysis algorithm, since local histogram presents bimodal behavior.

It is important to notice that if an array point does not belong to a foreign body, the local thresholding on the corresponding window will give a false recognition, while if any point of a foreign body is not included in the array, that corresponding body cannot be recognized. Thus the most important task is to determine a first threshold that provides a set of candidates including all the foreign bodies. Fig. 7 shows an example of this method for raisins contaminated with wooden sticks.

### *B. Statistical Analysis*

In the case of images with poor contrast and with foreign bodies having the same gray values as the food objects, adaptive binarization can not realize an efficient segmentation and identification of foreign bodies. To overcome this drawback, we implemented a method based on the interpretation of food product

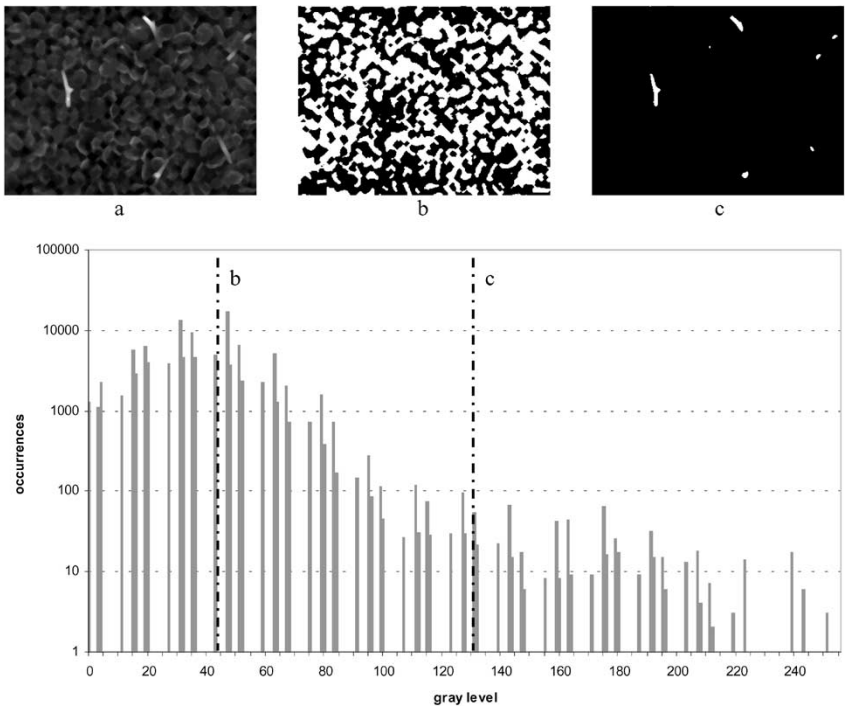


Fig. 6. Threshold level determination with non bimodal histogram: (a) original image, (b) binarization by discriminant or recursive methods (similar values), and (c) binarization by tail selection method. Note that $y$ axis has log scale.

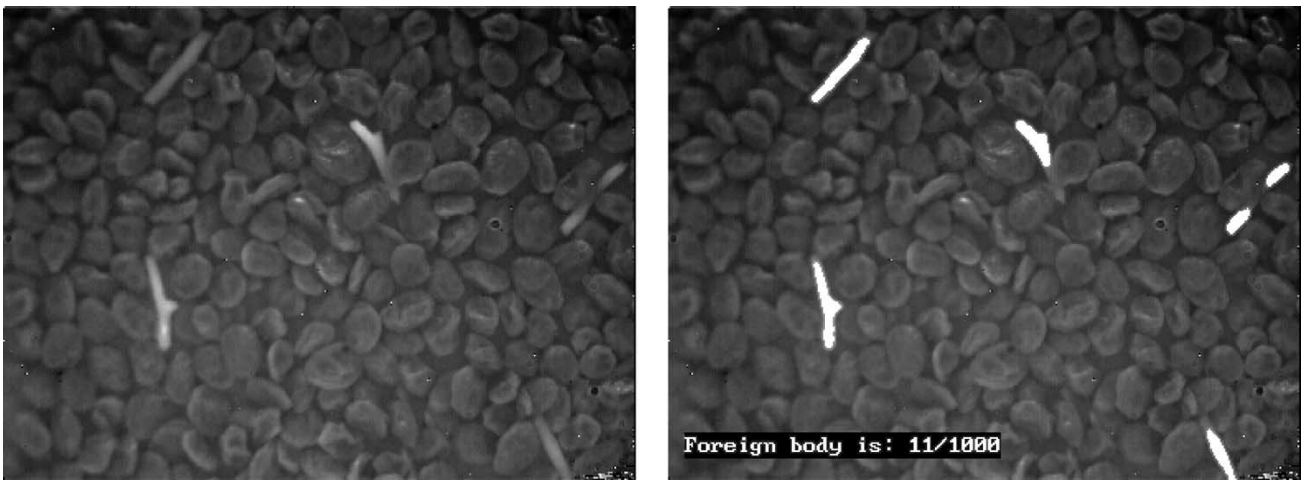


(a) (b)

Fig. 7. IR image of raisins and wooden sticks as (a) foreign bodies and (b) the recognized contaminants.

images as textures with spatially irregular repetitions of structural patterns and foreign bodies being the defects within this texture. Thus, we identified and measured some textural features able to enhance anomalies in a homogeneous behavior. Consequently, image portions containing foreign bodies can be identified.

Texture analysis can be performed in different ways; however, as our data clearly show random textures, the best approach is the statistical one. The algorithm we implemented starts by dividing images into blocks of fixed size. For each block, a texture feature (described below) is measured and compared with that of a prototype. After this, the blocks are classified by thresholding their distance values (Fig. 8).

The first problem to be solved relates to the size of blocks. It should not be too large, because it would be useless to segment images in wide regions containing not only foreign bodies but also a big part of the food product. On the other hand, each block has to be large enough to characterize the texture.

Another problem comes from image partitioning into blocks, that may result in spreading foreign bodies among adjacent blocks, and a consequent erroneous classification of those blocks as homogeneous. A simple way to solve this is to use overlapping blocks (as in Fig. 9), even if this results in a considerably higher computational load (at least four times).

Finally, a prototype texel has to be defined for comparison with each block. A simple and effective method is to use the

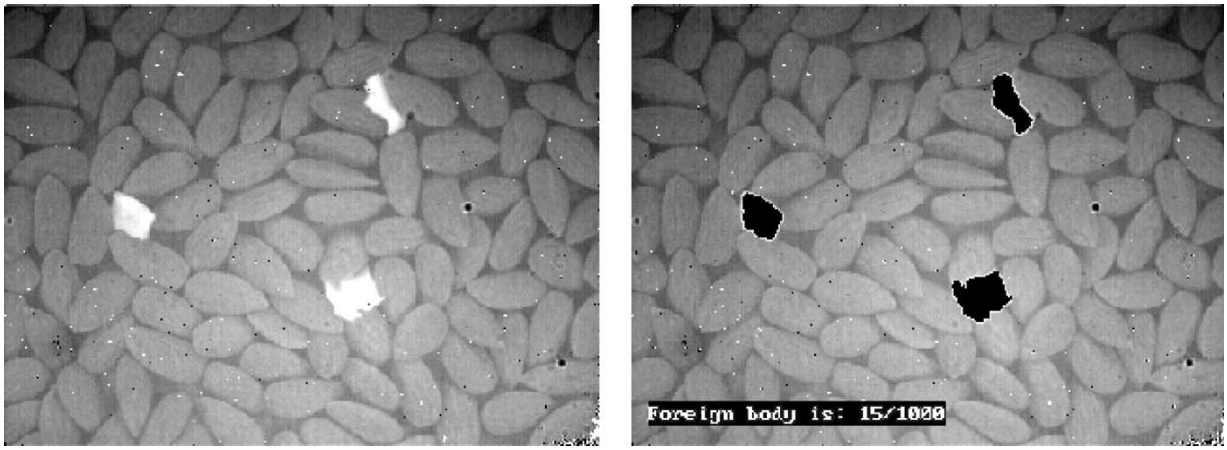


(a) (b)

Fig. 8. IR image of almonds and pieces of cardboard as (a) foreign bodies and (b) the recognized contaminants.

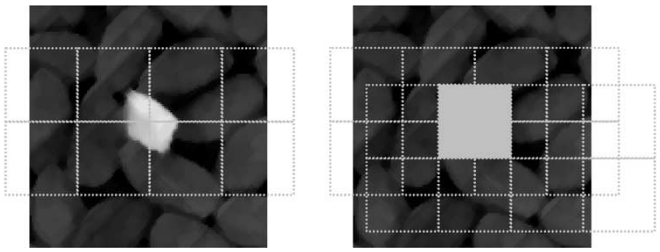

(a) (b)

Fig. 9. Effect of overlapping on a piece of cardboard within almonds. (a) Without overlapping, the object is spread among four blocks. Each block is erroneously classified as "good" since its statistics do not differ enough from the model. (b) With overlapping factor of 0.5, one block containing the whole foreign object is found. Its statistics are considerably different from the model and the block is correctly labeled as "bad."

whole image if the foreign bodies constitute a small percentage of it. Otherwise, the block with minimum square distance from all the other blocks can be used.

By taking into account real-time constraints, we devised a method based on histogram analysis (first-order statistics). Let us consider the gray level histogram $H(gl)$; the mean gray value $\overline{gl}$ is defined as

$$\overline{gl} = \frac{\sum_{gl=1}^{M} gl \cdot H(gl)}{\sum_{gl=1}^{M} H(gl)} \tag{5}$$

where $M$ is the total number of gray levels. The standard deviation is then

$$\sigma = \sqrt{\sum_{gl=o}^{M} \left(gl - \overline{gl}\right)^2 \cdot h(gl)} \text{ with } h(gl) = \frac{H(gl)}{\sum_{gl=1}^{M} H(gl)}. \tag{6}$$

We define three different metrics.

- *Mean value distance*

$$\overline{d} = \left(\overline{gl}_{\text{prototype}} - \overline{gl}_{\text{block}}\right)^2. \tag{7}$$

- *Mean and standard deviation distance*

$$d_{\mu\sigma} = \left(\overline{gl}_{\text{prototype}} - \overline{gl}_{\text{block}}\right)^2 + \left(\sigma_{\text{prototype}} - \sigma_{\text{block}}\right)^2. \tag{8}$$

- *Patrick–Fisher distance*

$$d_{\text{PF}} = \sum_{gl=1}^{M} \left(H_{\text{prototype}}(gl) - H_{\text{block}}(gl)\right)^2. \tag{9}$$

A good metric should present the following characteristics:

1) to be zero if and only if the two histograms are equal;
2) to be proportional to the distortion of the histogram's values;
3) to weight point-to-point differences according to their distance from the mean value.

The third condition is not satisfied by any of the proposed metrics; however, this will not affect the estimation unless two histograms to be compared present very similar shapes, with a slight displacement of a group of pixels only.

To define a metric that meets all the previous requirements, we used the rank-order statistics [13], [14]. For a block of $N$ pixels, quantized to $M$ levels, the rank function $R_H(Z)$ of the corresponding histogram $H(gl)$ is defined as the ordered ascending sequence of gray levels

$$R_H : [x] \rightarrow [y] \tag{10}$$

where $x \in [1, \ldots, N]$ is the position of a pixel in the ordered sequence, and $y \in [1, \ldots, M]$ is the corresponding gray level. It can be proven that there is a one-to-one equivalence between a rank function and its related histogram. Furthermore, to compare two rank functions with different cardinalities, functions must be normalized. By using these rank functions, the integral absolute error distance is defined

$$d_{IAE} = \int_0^1 \left| R_{H_{\text{prototype}}}(z) - R_{H_{\text{block}}}(z) \right| dz. \tag{11}$$

We selected the following distance between a textured block and a prototype:

$$d = \max\left(d_{\mu\sigma}, d_{IAE}\right) \tag{12}$$

where $d_{\mu\sigma}$ is as in (8) and $d_{IAE}$ as in (11).

It must be noticed that the processing time for this method is considerably longer than that for the adaptive binarization. While in the first case the algorithm is well suited for real-time

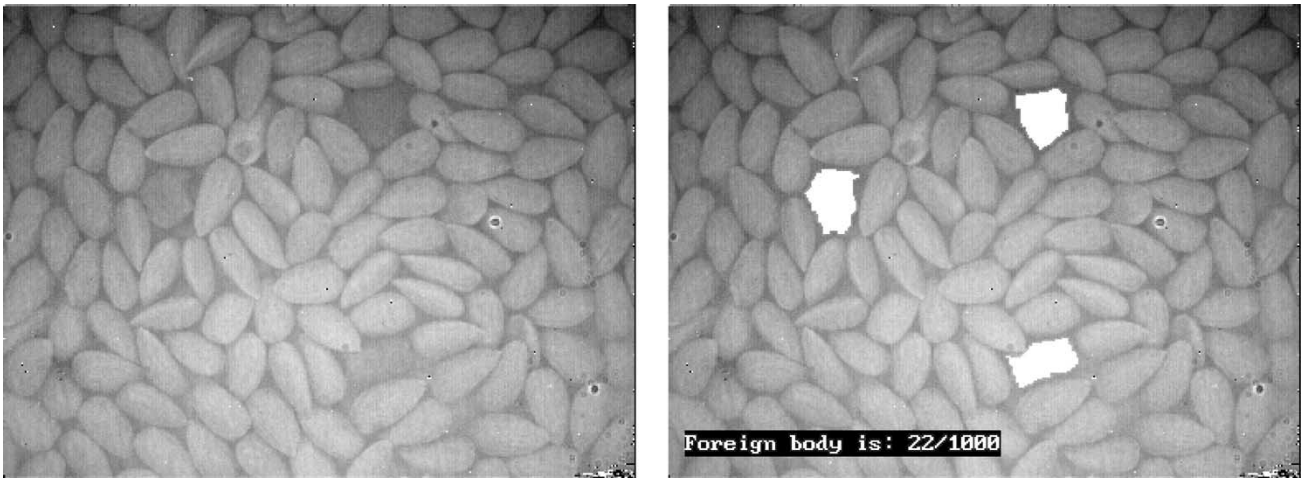


(a) (b)

Fig. 10. IR image of almonds and stones as (a) foreign bodies and (b) the recognized contaminants.

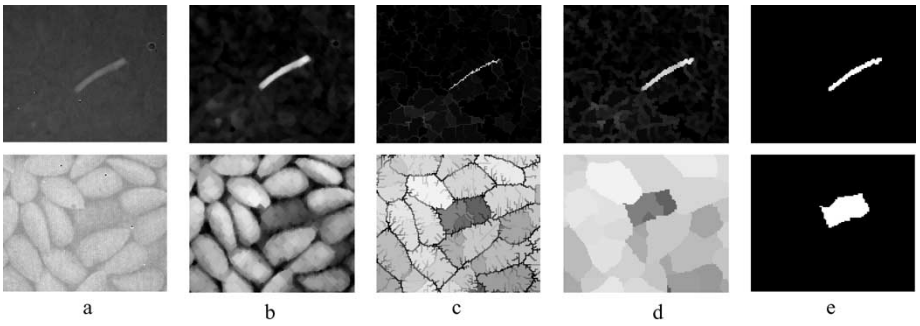


Fig. 11. IR images of raisins and wooden sticks (top) and almonds and stones as foreign bodies (bottom): (a) original IR image, (b) pre-processed image, (c) result of skeletonization, (d) dilated image, and (e) final result after region merging and thresholding.

implementation, block partitioning and iterated processing require more processing time. If we look, for instance, at the histogram computation, given a square image of size $N$, the adaptive binarization requires $N \times N + o(n \times n)$ summations, being $o$ the number of objects and $n$ the size of the local window. A typical situation would be $o = 3$ and $n = N/10$ thus resulting in $1.03N^2$ operations. The statistical approach with overlapping factor of *0.5* approximately requires $5N^2$ operation. Nonetheless, the task could be parallelized for faster execution.

### C. Morphological Analysis

The third approach we implemented is a method using mathematical morphology [11]. This approach was especially designed to meet the problem with small parts of food or background with the same gray level as foreign bodies, where binarization and statistical approaches may fail. The processing starts with a gray level skeletonization (thinning), followed by a gray level opening, so that a region segmentation is obtained. Small undesired details, such as areas from the background between objects, are deleted and a binary food/foreign-body representation can be obtained by region merging and thresholding (Fig. 10).

The requirements for a skeletonization procedure of binary objects can be defined very clearly [11]. In the case of gray level instead of binary images, the skeletonization rules have to be interpreted in a weak sense, as e.g., the curve thickness and the topology-preserving properties cannot be defined exactly for gray level images. We realized the gray level skeletonization through morphological operators where the skeletonization rules are used as qualitative principles.

Two cases must be considered, i.e., when foreign bodies are brighter or darker than the background (i.e., the homogeneous food product). In the former case, skeletonization can be achieved by thinning the white to idempotence, while in the latter by thinning the black to idempotence (Fig. 11); this is equivalent to thickening the white to idempotence. By defining a neighborhood and a structuring element as in Fig. 12, grayscale thinning can be defined as follows:

$$\text{if } [\text{MAX } (0) < \text{center pixel} <= \text{MIN}(1)] \text{ then center pixel} = \text{MAX}(0), \text{else center pixel unchanged.}$$

The grayscale thickening procedure is

$$\text{if } [\text{MAX } (0) <= \text{center pixel} < \text{MIN}(1)] \text{ then center pixel} = \text{MIN}(1), \text{else center pixel unchanged}$$

where $\text{MIN}(1)$ is the minimum of all pixels in the neighborhood that overlap with the structuring element, while $\text{MAX}(0)$ is the maximum of all remaining pixels in the neighborhood.

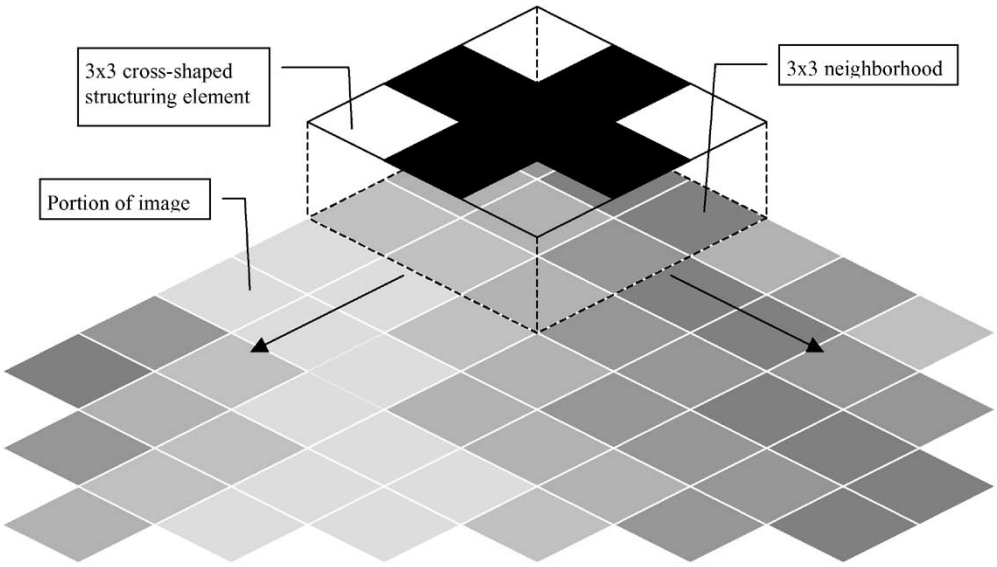


Fig. 12. Structuring element and neighborhood definition for the morphological processing.

## VI. Experimental Results

For the evaluation of our methods we used ten different test images, which we acquired with a thermographic camera in an experimental environment. Eight of these images present bright foreign bodies on a more or less structured dark background created by the food objects. In two cases the foreign bodies are darker than most of the surrounding food objects. The results we achieved are of course not representative but they give a first impression of the usefulness of the proposed method. Of course, experiments with images coming from the real production process have to follow. The foreign body recognition results are evaluated using three features:

- the ratio between *recognized* and *misrecognized* foreign bodies, where *recognized* means foreign bodies present in the original data, and *misrecognized* means food objects recognized as foreign bodies;
- the ratio between foreign body area in original (interactively measured) and processed data; in this latter case, area relates to the number of pixels in recognized and misrecognized foreign bodies;
- the recognized object connectivity; this can be regarded as a quality index for processing, even if shape information is not essential for foreign body recognition at this stage.

A quality index (QI) that takes into account the previous factors, weighted appropriately on account of their relative importance for our task, was defined

$$QI = q_{\text{objects}} + q_{\text{area}} + q_{\text{connectivity}} \tag{13}$$

where definitions are given in (14)–(16), shown at the bottom of the page. The results in Fig. 13 show good quality QI values. It must be noted that QI values are not representative by themselves, but as comparison between different approaches.

For most of the ten test images the three recognition methods give more or less the same performance. Even though the local method provides the best results in six cases, only in one case there is a noticeable difference to the QI of the second best method. On the other hand, the local method is the worst method in one case. The statistical and the morphological method are the best of all in one case. The local method is generally preferable thanks to its average good performance and its low computational cost. Nonetheless, in case of poorly contrasted images, such as almonds and metal chips (see also Fig. 4), the statistical method could give better results, especially if optimized for particular class of products.

$$q_{\text{objects}} = 0.7 \cdot \left( \frac{N_{\text{recognizedobjects}}}{N_{\text{originalobjects}}} - \frac{N_{\text{misrecognizedobjects}}}{N_{\text{originalobjects}}} \right) \tag{14}$$

$$q_{\text{area}} = \begin{cases} 0.2 \cdot \left( - \left( \frac{V_{\text{recognizedarea}}}{V_{\text{originalarea}}} \right)^2 + 2 \cdot \left( \frac{V_{\text{recognizedarea}}}{V_{\text{originalarea}}} \right) \right) & V_{\text{recognizedarea}} \leq 2 \cdot V_{\text{originalarea}} \\ 0 & V_{\text{recognizedarea}} > 2 \cdot V_{\text{originalarea}} \end{cases} \tag{15}$$

$$q_{\text{connectivity}} = 0.1 \cdot \frac{N_{\text{recognized connected objects}}}{N_{\text{originalobjects}}}. \tag{16}$$

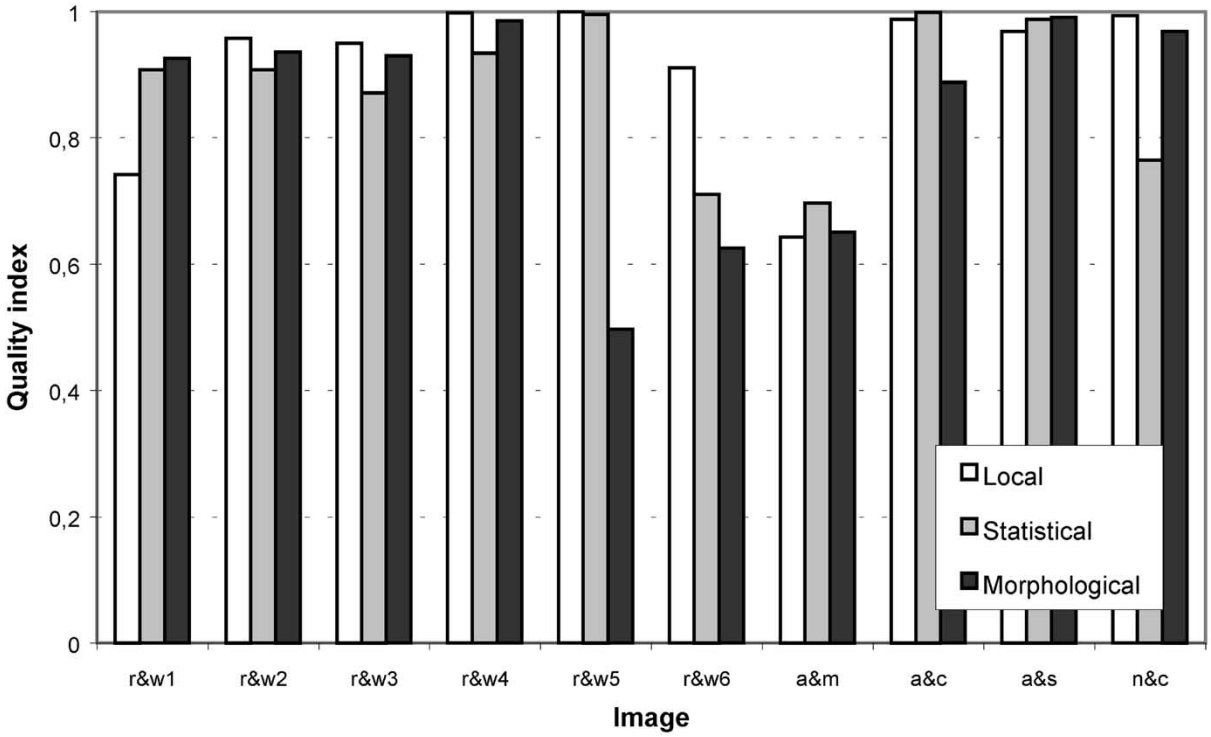


Fig. 13. Quality index histograms for each image and recognition method (legend: r&w = raisins + wooden sticks; a&m = almonds + metal chips; a&c = almonds + cardboard pieces; a&s = almonds + stones; n&c = nuts + cardboard pieces ).

These first results show that the proposed recognition methods are well adapted to the problem of detecting foreign bodies in food using IR thermography.

## VII. Conclusion

We introduced a concept for using thermographic images for detecting foreign bodies in the food industry. Different processing approaches were developed and illustrated to cope with several cases, even if at this preliminary stage, a common working framework is still missing (i.e., processing needs for some interaction by the operator).

Image processing algorithms, based on local thresholding, rank order statistics and morphological operators demonstrated good performance in a variety of cases.

Nonetheless, the methods have to be implemented in a system and even then, an optimization and integration process has to follow, aiming at obtaining an autonomous nondestructive visual inspection tool for food products.

## References

[1] T. C. Pearson, M. Doster, and T. J. Michailides, "Automated detection of pistachio defects by machine vision," *Appl. Eng. Agri.* , vol. 17, no. 5, pp. 81–84, 2001.

[2] A. Talukder, D. Casasent, H. Lee, P. M. Keagy, and T. F. Schatzki, "New feature extraction method for classification of agricultural products from X-ray images," in *Proc. SPIE Precision Agriculture and Biological Quality*, vol. 3543, 1 1999, pp. 119–130.

[3] D. Casasent, M. A. Sipe, T. F. Schatzki, P. M. Keagy, and L. L. Lee, "Neural net classification of X-ray pistachio nut data," *Lebensmittel-Wissenschaft Und-Technol.*, vol. 31, pp. 122–128, 1998.

[4] T. C. Pearson, "Use of near infrared transmittance to automatically detect almonds with concealed damage," *Lebensmittel-Wissenschaft Und-Technol.*, vol. 32, no. 2, pp. 73–78, 1999.

[5] A. D. Mowat and P. R. Poole, "Non-destructive discrimination of persimmon fruit quality using visible-near-infrared reflectance spectro-photometry," *Acta Horticulture (ISHS)*, vol. 436, pp. 159–163, 1997.

[6] G. Gaussorgues, *Infrared Thermography*. London, U.K.: Chapman & Hall, 1994.

[7] S. M. Sze, *Semiconductor Sensors*. New York: Wiley, 1994.

[8] X. P. V. Maldague, *Nondestructive Evaluation of Materials by Infrared Thermography*. Berlin, Germany: Springer-Verlag, 1993.

[9] *Thermosensorik System CMT 384 M Manual*, Thermosensorik GmbH, Erlangen, Germany, 2000.

[10] P. Wallin and P. Haycock, *Foreign Body Prevention, Detection and Control*. Glasgow, U.K.: Blackie, 1998.

[11] J. Serra, *Image Analysis and Mathematical Morphology*. New York: Academic, 1988.

[12] N. Otsu, "A threshold selection method from gray-level histograms," *IEEE Trans. Syst., Man, Cybern.*, vol. SMC-9, pp. 62–66, Jan. 1979.

[13] F. G. B. DeNatale, "Rank-order functions for the fast detection of texture faults," *Int. J. Pattern Recognit. Artif. Intell.*, vol. 10, no. 8, pp. 971–984, 1996.

[14] P. Zamperoni, "Feature extraction by rank-order filtering for image segmentation," *Int. J. Pattern Recognit. Artif. Intell.*, vol. 2, no. 2, pp. 301–319, 1988.

[15] T. W. Ridler and S. Calvard, "Picture thresholding using an iterative selection method," *IEEE Trans. Syst., Man, Cybern.*, vol. 8, pp. 630–632, Aug. 1978.

**Giaime Ginesu** (S'04) graduated in electronic engineering (M.S. degree) in 2001 from the University of Cagliari, Cagliari, Italy, where he is currently working toward the Ph.D. degree in the CNIT Multimedia Communications Laboratory, Department of Electrical and Electronic Engineering.

He is also a member of the CNIT's Unit of Research. He spent six months at the Institute for Telecommunications of the Technical University of Braunschweig, Germany, to work on his Masters thesis under an Erasmus Grant. His thesis concerned thermal image processing and recognition. His research interests are related to image processing and transmission, volumetric image processing, and JPEG2000/MPEG standards. He is a participant in the 2KAN (JPEG 2000 Advanced Networking) European Union project. In 2003, he spent six months at Rensselaer Polytechnic Institute, Troy, NY, as a Visiting Scholar.

**Daniele D. Giusto** (S'87–M'90–SM'00) received the Laurea (M.S.) degree in electronic engineering and the Dottorato di Ricerca (Ph.D.) degree in telecommunications from the University of Genoa, Genoa, Italy, in 1986 and 1990, respectively.

Since 1994, he has been a permanent faculty member in the Department of Electrical and Electronic Engineering, University of Cagliari, Cagliari, Italy, where he became Full Professor of Telecommunications in 2002. In 1995 and 1998, he was a Visiting Professor at the Institute for Telecommunications, Technical University of Braunschweig, Germany. His research interests are in the areas of image and video processing and coding, multimedia systems, digital television, pictorial databases, and personal communications.

Dr. Giusto is a Member of the Executive Board of CNIT, the Italian University Consortium for Telecommunications. He was the recipient of the 1993 AEI Ottavio Bonazzi Best Paper Award and co-recipient of the 1998 IEEE Chester Sall Best Paper Award. Since 1999, he has been acting as the Head of the Italian delegation within the ISO-JPEG international standardization committee. He has been a Guest Editor for several journals and acted as General Chair for the PACKET VIDEO 2000 International Workshop and the 1st International IEEE-SPIE Workshop on JPEG2000.

**Volker Märgner** (M'95) received the Diploma (Dipl.-Ing.) and Doctorate (Dr.-Ing.) degrees in electrical engineering from the Technical University Braunschweig, Braunschweig, Germany, in 1974 and 1983, respectively.

Since 1983, he has been working at the Technical University Braunschweig. Currently, he is a member of the research and teaching staff in the Institute for Communications Technology, Department of Signal Processing for Mobile Information Systems, in the position of an Akademischer Oberrat. His main areas of research are image processing and pattern recognition. Currently, he is working on image preprocessing and pattern recognition methods and their application to industrial quality control using visible light and thermography as well as to the recognition of cursive handwriting on paper documents. He has authored more than 30 published technical papers in his research areas.

Dr. Märgner is a member of the VDE/VDI.

**Peter Meinlschmidt** studied physics at the University of Hamburg, Hamburg, Germany, the University of Oldenburg, Oldenburg, Germany, and Towson State University, Towson, MD, where, as a member of the Applied Optics Group in the Physics Department, he received the M.S. degree in 1991 in the field of holographic recording of 3-D flows.

He then worked in the same group on applications of video holography (ESPI) to historical monuments. Since 1996, he has been with the Fraunhofer Institute for Wood Research, Braunschweig, Germany, working on NDE applications of thermography and video holography to organic and inorganic materials. His current research interests include optical metrology, thermography, holography, and image processing techniques.